

#### **OPEN ACCESS**

EDITED BY Steven Kregel, Loyola University Chicago, United States

REVIEWED BY
Ritika Tiwari,
University of Miami, United States
Paula Dobosz,
Poznan University of Medical Sciences, Poland

\*CORRESPONDENCE

Xiao Xiao

⊠ dr.xiaoxiao@stu.cqmu.edu.cn

Yuhua Mei

<sup>†</sup>These authors have contributed equally to this work

RECEIVED 14 August 2025 REVISED 31 October 2025 ACCEPTED 07 November 2025 PUBLISHED 21 November 2025

#### CITATION

Hu X, Xie T, Xiao X and Mei Y (2025) LncRNA *ELDR* promotes bladder cancer malignant progression by regulating the miR-1343-3p/*TRIM44* axis. *Front. Oncol.* 15:1685792. doi: 10.3389/fonc.2025.1685792

#### COPYRIGHT

© 2025 Hu, Xie, Xiao and Mei. This is an openaccess article distributed under the terms of the Creative Commons Attribution License (CC BY). The use, distribution or reproduction in other forums is permitted, provided the original author(s) and the copyright owner(s) are credited and that the original publication in this journal is cited, in accordance with accepted academic practice. No use, distribution or reproduction is permitted which does not comply with these terms.

# LncRNA *ELDR* promotes bladder cancer malignant progression by regulating the miR-1343-3p/ *TRIM44* axis

Xiao Hu<sup>1,2†</sup>, Tianhang Xie<sup>2†</sup>, Xiao Xiao <sup>3\*</sup> and Yuhua Mei<sup>4,5\*</sup>

<sup>1</sup>Frontiers Science Center for Disease-related Molecular Network, Department of Orthopedic Surgery and Orthopedic Research Institute, West China Hospital, Sichuan University, Chengdu, Sichuan, China, 
<sup>2</sup>Department of Orthopedic Surgery and Orthopedic Research Institute, West China Hospital, Sichuan University, Chengdu, Sichuan, China, 
<sup>3</sup>Department of Urology, Chongqing University Fuling Hospital, Chongqing, China, 
<sup>4</sup>Department of Urology, The First Affiliated Hospital of Chongqing Medical University, Chongqing, China, 
<sup>5</sup>The First Affiliated Hospital of Chongqing Medical University, Chongqing, China

**Introduction:** Bladder cancer (BCa) is one of the most prevalent genitourinary malignancies with high recurrence worldwide. A lack of reliable prognostic biomarkers and effective therapeutic targets hinders its treatment. Emerging evidence indicates that long noncoding RNAs (IncRNAs) are involved in human cancers, including BCa. While IncRNAs hold enormous promise, their specific roles and mechanisms in BCa remain largely unexplored. Here, we identify the IncRNA ELDR as a pivotal oncogenic driver in BCa.

**Methods:** RT-qPCR was used to analyze the expression patterns of ELDR, miR-1343-3p and TRIM44. CCK-8, colony formation, EdU, and Transwell assays were used to detect the effect of ELDR on cell proliferation, migration, and invasion. The association between ELDR, miR-1343-3p and TRIM44 was analyzed by bioinformatics analysis and dual-luciferase reporter assay. Finally, the role of the ELDR-miR-1343-3p-TRIM44 axis in bladder cancer cell behavior was demonstrated.

Results and Discussion: ELDR is significantly upregulated in BCa tissues, and its high expression correlates with aggressive clinicopathological features and predicts poor prognosis in BCa patients. Functional experiments demonstrate that ELDR enhances BCa cell proliferation, colony formation, migration, and invasion in vitro and accelerates tumor growth in vivo. Mechanistically, ELDR functions as a competitive endogenous RNA (ceRNA) by sequestering tumor-suppressive miR-1343-3p in the cytoplasm, which consequently leads to the upregulation of the oncogene TRIM44. Our findings unveil the ELDR/miR-1343-3p/TRIM44 axis as a crucial pathway in BCa progression, establishing ELDR as a promising prognostic biomarker and an attractive candidate for the development of targeted therapies.

KEYWORDS

bladder cancer, ELDR, ceRNA, miR-1343-3p, TRIM44

#### 1 Introduction

Bladder cancer, ranking as the second most prevalent malignancy of the genitourinary system, accounts for over 573,000 new cases globally each year (1). The characteristics of frequent recurrence and metastasis are the main reasons for its poor prognosis (2). The past decade has been important for strides in BCa detection and management. However, the prognosis for most patients remains poor. High recurrence rates and the aggressive course of disease mean an undesirable 5-year survival rate of BCa (3). Therefore, identifying novel genes and pathways involved in BCa is critical for developing new diagnostic and therapeutic approaches.

Long non-coding RNAs (lncRNAs) are defined as transcripts longer than 200 nucleotides with limited protein-coding potential. They have emerged as critical regulators of gene expression and cellular homeostasis (4). Although initially considered "transcriptional noise", recent studies reveal that lncRNAs participate in diverse biological processes, including chromatin remodeling, RNA stability modulation, and signal transduction cascades. Interactions with proteins, DNA, or other RNAs enable these functions (5, 6). The roles of lncRNAs in disease pathogenesis -particularly cancer-are increasingly recognized. Numerous dysregulated lncRNAs operate as competitive endogenous RNAs (ceRNAs). They contribute to tumor initiation, metastasis, and therapy resistance by sponging tumor-suppressive miRNAs and derepressing oncogenic target genes (7, 8). For example, Xue et al. revealed that lncRNA LUESCC is highly expressed in ESCC and acts as a ceRNA to promote tumor proliferation, invasion, and migration by targeting the miR-6785-5p/NRSN2 axis (9). Furthermore, Sheng et al. observed a clear upregulation of LINC01980 in HCC, which they correlated with a poor prognosis (10). Despite its association with various cancers, the role of lncRNA ELDR in BCa remains unclear. A previous study on oral cancer demonstrated that ELDR enhances tumor growth by promoting ILF3-cyclin E1 signaling (11). Additionally, ELDR is highly expressed and has potential as a biomarker of poor prognosis in the serum extracellular vesicles of breast cancer patients (12). These findings support the role of *ELDR* as an oncogenic molecule, suggesting the need for further studies on its mechanistic role in bladder carcinogenesis progression.

MicroRNAs (miRNAs) are small non-coding RNAs of 21–25 nucleotides. They are master regulators of carcinogenesis, modulating oncogenes and tumor suppressors at the post-transcriptional level (13). In BCa, dysregulated miRNAs drive malignant phenotypes—including proliferation, migration, invasion, and therapy resistance—through interactions with key genes (14, 15). For instance, Zhang et al. displayed that miR-15b-3p-mediated inhibition of ferroptosis could weaken bicalutamide sensitivity in prostate cancer (16). As a tumor suppressor gene, miR-1343-3p has been reported to be downregulated in expression in a variety of malignancies (17–19). Notably, Lai et al. revealed that miR-1343-3p can serve as an early screening marker for BCa (20). However, the potential mechanism of miR-1343-3p in BCa needs to be further explored.

Tripartite motif-containing 44 (TRIM44), a cytoplasmic and nuclear regulatory protein (21), is dysregulated in multiple human malignancies. Previous research indicated elevated TRIM44 levels in ovarian cancer drive tumor progression via activating the NF-kB pathway (22). It also correlates with aggressive clinical behavior in prostate cancer (23). A previous study demonstrated that TRIM44 was a risk factor affecting BCa (24); however, the underlying mechanism by which TRIM44 regulated BCa development remained unclear.

In this investigation, we demonstrate that highly expressed *ELDR* promotes malignant progression of BCa by targeting the miR-1343-3p/*TRIM44* axis, which is correlated with the poor prognosis. Therefore, *ELDR* may serve as a diagnostic biomarker and therapeutic target for BCa patients.

#### 2 Materials and methods

#### 2.1 Clinical tissue specimens collection

Primary BCa tumor tissues and paired adjacent normal tissues (at least 3 cm from the edge of cancer tissues) were acquired from 58 treatment-naïve patients undergoing curative resection at the First Affiliated Hospital of Chongqing Medical University (2019-2021). All cases received histopathological confirmation by two independent pathologists, with exclusion criteria encompassing any preoperative anticancer therapy. Immediately following surgical excision, tissues were snap-frozen in liquid nitrogen and cryopreserved at -80°C for molecular analyses. The study protocol obtained formal approval from the Medical Ethics Committee of the First Affiliated Hospital of Chongqing Medical University (2021-199), with written informed consent procured from all participants.

#### 2.2 Cell culture and treatment

The human urothelial cell lines (SV-HUC-1, J82, T24, UM-UC-3, 5637, and RT4) were obtained from Wuhan Procell Biotechnology (Wuhan, China). Cells were maintained at 37°C in a humidified 5% CO<sub>2</sub> incubator using the following media: SV-HUC-1 in F12K basal medium (Gibco, USA), J82 and UM-UC-3 in Dulbecco's modified eagle media (DMEM, Gibco, USA), and T24/5637/RT4 in RPMI-1640 (Gibco, USA). All media contained 10% bovine serum (FBS; Procell, Wuhan, China) and 1% penicillin/streptomycin (Sangon, Shanghai, China).

## 2.3 Cell transfection, plasmids and oligonucleotides

Overexpression constructs for *ELDR* (pcDNA3.1-*ELDR*) and *TRIM44* (pcDNA3.1-TRIM44), along with *ELDR*-targeting shRNA (sh-*ELDR*) and miR-1343-3p mimics/inhibitors, were procured from Tsingke Biotechnology (Beijing, China). Corresponding

negative control vectors and oligonucleotides were included. For gene modulation, cells were transfected using Lipofectamine TM 3000 (Invitrogen, USA) per the manufacturer's protocol, with plasmid validation via Sanger sequencing.

## 2.4 RNA isolation, reverse transcription, and RT-qPCR

Total RNA isolation from cells and clinical specimens was performed with TRIzol reagent (Abclonal, China). The purified RNA underwent reverse transcription using the PrimeScript qRT-PCR kit (Abclonal, China). Subsequently, qRT-PCR analysis was conducted using the SYBR(R) Prime-Script RT-PCR kit (Abclonal, China) on an ABI 7500 Real-Time PCR Platform (Applied Biosystems, USA). Actin and U6 were used as internal controls, and gene expression levels were normalized to internal controls and quantified via the 2-ΔCt method. All samples were run in triplicate.

## 2.5 Cell counting kit-8 and colony formation assay

Cells were plated in 96-well plates at a density of  $3\times10^3$  cells per well. After incubation for 6 h, 24 h, 48 h, 72 h, and 96 h, the CCK-8 reagent (10 µL, Sangon) was incubated with each well for 1 h at 37°C, 5% CO<sub>2</sub>. Absorbance was measured at 450 nm using a microplate reader (Thermo Fisher, USA). About the colony formation assay, cells (1.5  $\times$  10³/well) were seeded in 6-well plates and incubated at 37°C, 5% CO<sub>2</sub> until colonies were visible. The cells were then fixed with 4% paraformaldehyde and stained with 0.1% crystal violet, and the colonies were counted.

#### 2.6 Transwell migrating and invasion assay

For migration assays, cells were seeded in RPMI-1640 (500  $\mu$ L) at  $1\times10^4$  density in the upper chamber of Transwell inserts, with DMEM containing 10% FBS (1000  $\mu$ L) in the lower compartment. Following 12 h incubation, migrated cells were fixed and stained with 0.1% crystal violet (30 min), then imaged using a microscope (Thermo Fisher, USA). Invasion assays followed identical procedures except for Matrigel coating (Corning; 1:8 dilution in serum-free medium) applied to the upper membrane prior to cell seeding.

#### 2.7 Proliferation assay

Cell proliferation was assessed using an EdU Cell Proliferation Kit (C0071S, Beyotime), following the manufacturer's protocol. Briefly, cells  $^4y$  of  $4{\times}10^4$  cells per well and pretreated for 24 hours. Subsequently, half of the medium was replaced with EdU-containing buffer (20  $\mu M$ ) for a 3-hour incubation period. Following fixation and permeabilization, the cells were incubated

with click reaction solution and DAPI (1:1000 dilution). Three randomly selected fields per well were imaged, and the results were averaged for statistical analysis.

#### 2.8 Western blot assay

Total protein was isolated from cells and tissues using RIPA lysis buffer (Beyotime) supplemented with phenylmethanesulfonyl fluoride (PMSF) at a 1:100 ratio. Following separation by SDS-PAGE, proteins were transferred onto PVDF membranes (EMD Millipore). The membranes were blocked for 1 hour in Trisbuffered saline (TBS) containing 5% skim milk and then incubated overnight at 4 °C with the following primary antibodies: PCNA (Proteintech, 10205-2-AP), GAPDH (Proteintech, 60004-1-Ig), TRIM44 (Abcam, ab236422), and  $\beta$ -actin (Proteintech, 66009-1-Ig). After washing, membranes were exposed to a species-matched secondary antibody for 1 hour at room temperature. Protein signals were finally detected using enhanced chemiluminescence (Cell Signaling Technology, USA).

#### 2.9 Subcellular fractionation

Nuclear and cytoplasmic fractions were prepared from BCa cells cultured on 15 cm plates. Following two washes with ice-cold PBS, cells were gently scraped into a 15 mL Falcon tube. The resulting cell pellet was resuspended in 1 mL of hypotonic buffer (10 mM HEPES pH 8.0, 1.5  $\mu$ M MgCl<sub>2</sub>, 10 mM KCl, 1  $\mu$ M DTT) and incubated on ice for 15 minutes to induce cell swelling. After that, NP-40 was then added to the suspension to a final concentration of 1%, followed by brief vortexing (10 seconds) and centrifugation at 12,000 rpm for 2-3 minutes; the supernatant constituted the cytoplasmic fraction, while the pellet represented the nuclear fraction. Total RNA or protein from each compartment was subsequently extracted using Trizol (Abclonal, China) or RIPA lysis buffer (Beyotime), respectively, according to the manufacturers' instructions. ELDR expression patterns across cellular fractions were assessed by RT-qPCR, using actin and U6 as internal controls for cytoplasmic and nuclear RNA, respectively. Finally, fraction purity was validated by immunoblotting with anti-GAPDH and anti-PCNA antibodies serving as cytoplasmic and nuclear markers, respectively.

#### 2.10 Tumor xenograft in vivo

Six-week-old male BALB/c nude mice were randomly divided into three groups (n=5) and housed under SPF conditions. For xenograft experiments, T24 cells stably transfected with lentiviral vectors for shRNA against ELDR (1 × 10^6/100  $\mu$ L) were injected subcutaneously into the back of nude mice. Tumor. Tumor size was assessed for three consecutive weeks, and after 21 days the mice received intraperitoneal pentobarbital (150 mg/kg). Death was confirmed by cervical dislocation, and the tumor tissue was

weighed. The animal experiments were approved by the Ethics Committee of the First Affiliated Hospital of Chongqing Medical University.

#### 2.11 Immunohistochemistry

Tumor specimens were fixed in 10% paraformaldehyde, decalcified with formic acid, and paraffin-embedded. Consecutive 4-µm sections were cut and subjected to deparaffinization and antigen retrieval (Dako, CA, USA). After blocking with goat serum, avidin, and biotin solutions, sections were incubated overnight with anti-Ki67 primary antibody (Abcam, 1:200, ab15580), followed by 1-hour incubation with secondary antibody (Abcam, 1:500, ab150077). Stained sections were finally examined under an inverted microscope (Nikon, Tokyo, Japan).

#### 2.12 Dual luciferase reporter assay

The potential binding site between *ELDR* and miR-1343-3p was predicted using the starBase online database. A fragment of the human *ELDR* gene containing this site was amplified by PCR. Site-directed mutagenesis was performed on the predicted miR-1343-3p binding site within this fragment using a dedicated kit (Stratagene, USA). The resulting wild-type (wt) and mutant (mut) *ELDR* sequences were cloned into the PGL3 vector (GenePharma) to generate *ELDR*-wt-luc and *ELDR*-mut-luc reporter plasmids. Cells were then co-transfected with either *ELDR*-wt-luc or *ELDR*-mut-luc plasmids together with miR-1343-3p mimics or negative control mimics (NC), using Lipofectamine TM 3000 (Invitrogen). Luciferase activity was measured 48 hours post-transfection using the Dual-Luciferase Reporter Assay System (Promega, WI, USA), following the manufacturer's instructions. This identical experimental approach was applied to confirm the interaction between miR-1343-3p and *TRIM44*.

#### 2.13 AGO2-RIP and MS2-RIP

The Magna RIP Kit (Millipore, USA) was used for RNA immunoprecipitation (RIP) experiments in accordance with product guidelines. 5 µg of control IgG or anti-Argonaute 2 (AGO2) antibody (Abcam, USA) was added to pre-cleared BCa cell lysates in RIP lysis solution, which were then rotated and incubated for an entire night at 4 °C. After adding protein A/G magnetic beads to separate RNA-protein complexes, bound RNAs were released by proteinase K digestion. Using quantitative real-time PCR, the quantities of precipitated target RNA were measured.

For MS2-RIP validation of endogenous lncRNA-*ELDR*/miR-1343-3p binding, wild-type lncRNA-*ELDR* and its miR-1343-3p binding-site mutant were cloned into pcDNA3.1-MS2 (12×) to create pcDNA3.1-MS2-*ELDR*-WT and pcDNA3.1-MS2-*ELDR*-MUT constructs for MS2-RIP validation of endogenous lncRNA-*ELDR*/miR-1343-3p binding. In addition to pcDNA3.1-MS2/GFP (expressing MS2-GFP fusion protein), BCa cells were co-transfected

with pcDNA3.1-MS2 (vector control), pcDNA3.1-MS2-*ELDR*-WT, or pcDNA3.1-MS2-*ELDR*-MUT. Using the previously indicated RIP technique, RNA complexes were immunoprecipitated with anti-GFP antibody (Abcam, USA) during a 48-hour incubation period.

#### 2.14 Statistical analysis

Data from at least three independent experiments are expressed as mean  $\pm$  SD and analyzed using GraphPad Prism 9.5.1. Group comparisons employed Student's t-test (two groups) or one-way ANOVA (multiple groups). Associations between *ELDR* expression and clinicopathological features were assessed by the chi-square test. Survival distributions were analyzed with Kaplan-Meier curves and log-rank testing. Correlation analyses used Pearson's coefficients. All tests were two-tailed, with \*p\* < 0.05 considered statistically significant.

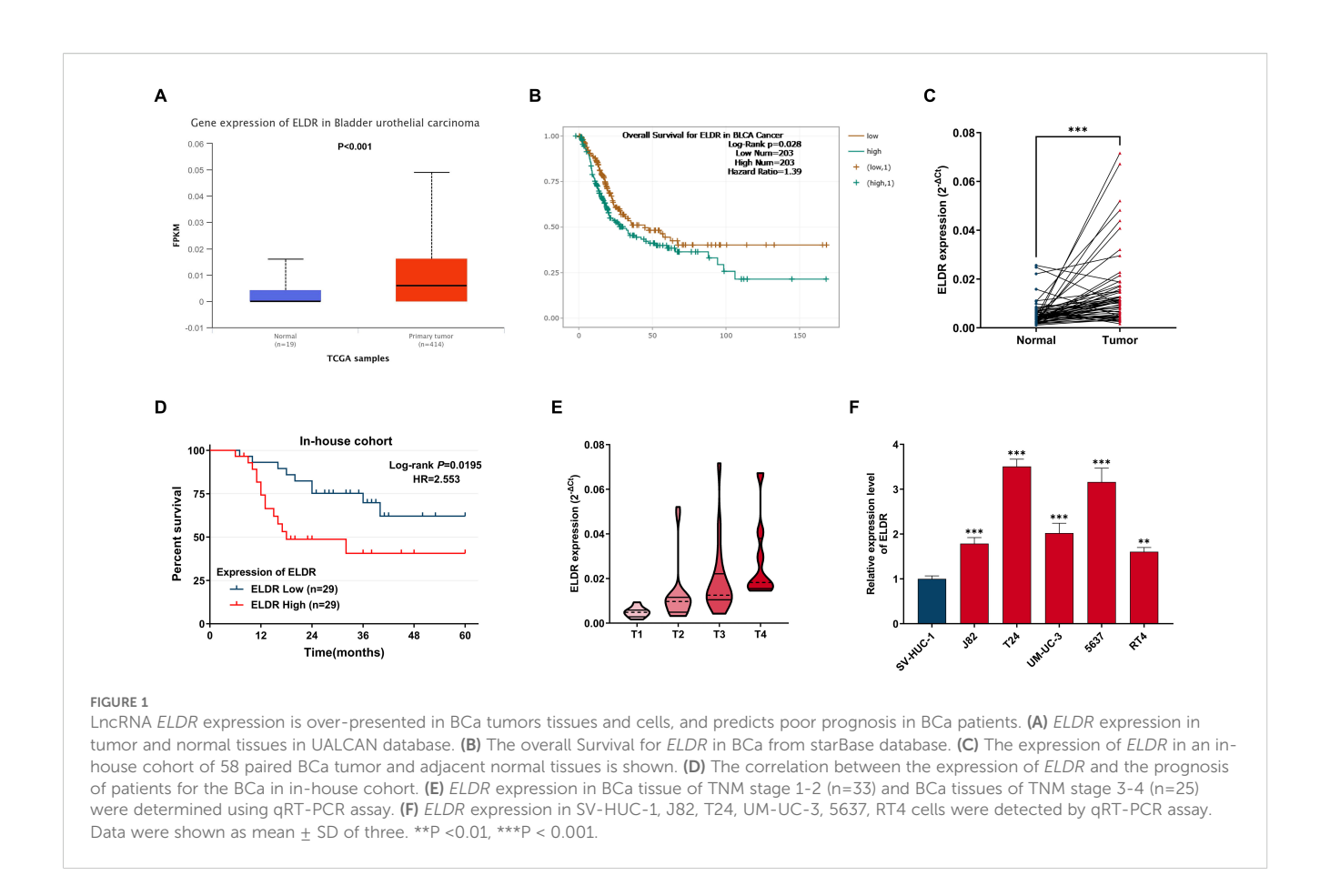
#### 3 Results

# 3.1 *ELDR* is significantly upregulated in BCa tissues and cell lines, correlating with poor prognosis

To explore the correlation of ELDR with BCa development, we analyzed its expression in TCGA-BCa data via the UALCAN web portal. As shown in Figure 1A, ELDR expression was substantially upregulated in BCa tissues compared to normal tissues. Subsequently, using the starBase database, we found that high ELDR levels were markedly associated with poor prognosis in BCa patients (Figure 1B). To validate these findings and further strengthen the clinical significance of ELDR, we obtained tumor tissues and paired adjacent normal tissues from 58 bladder cancer patients. The result of the qRT-PCR assay suggested that the ELDR expression was obviously elevated in BCa tissues (Figure 1C, Supplementary Table S1). Moreover, we found that higher ELDR levels predicted a worse prognosis and enhanced malignant progression (Figures 1D, E, Supplementary Table S1). Multivariate analysis of clinicopathological characteristics identified that high levels of ELDR were independently associated with tumor size, tumor invasion depth, and TNM stage within our cohort (Supplementary Table S2). Consistently, qRT-PCR analysis confirmed that ELDR levels were markedly higher in BCa cell lines (J82, T24, UM-UC-3, 5637, and RT4) than in the normal uroepithelial sv-HUC-1 line (Figure 1F). In summary, these results suggested that ELDR was pronouncedly elevated in BCa tissues and cell lines, correlating with clinicopathological features.

### 3.2 *ELDR* promotes BCa cells malignant behaviors *in vitro*

To investigate the potential biological functions of *ELDR* in BCa progression, we performed gain- and loss-of-function experiments.



Transfection with pcDNA3.1-ELDR significantly increased ELDR levels in both T24 and 5637 cells, while sh-ELDR transfection effectively reduced its expression (Figure 2A). Subsequently, we performed CCK-8, colony formation, transwells and EdU assays *in vitro*. As shown in Figures 2B-E, ELDR knockdown substantially inhibited proliferation, colony formation, migration, and invasion in both cell lines, whereas its overexpression potentiated these malignant phenotypes. Taken together, ELDR promotes the malignant behaviors of BCa cells.

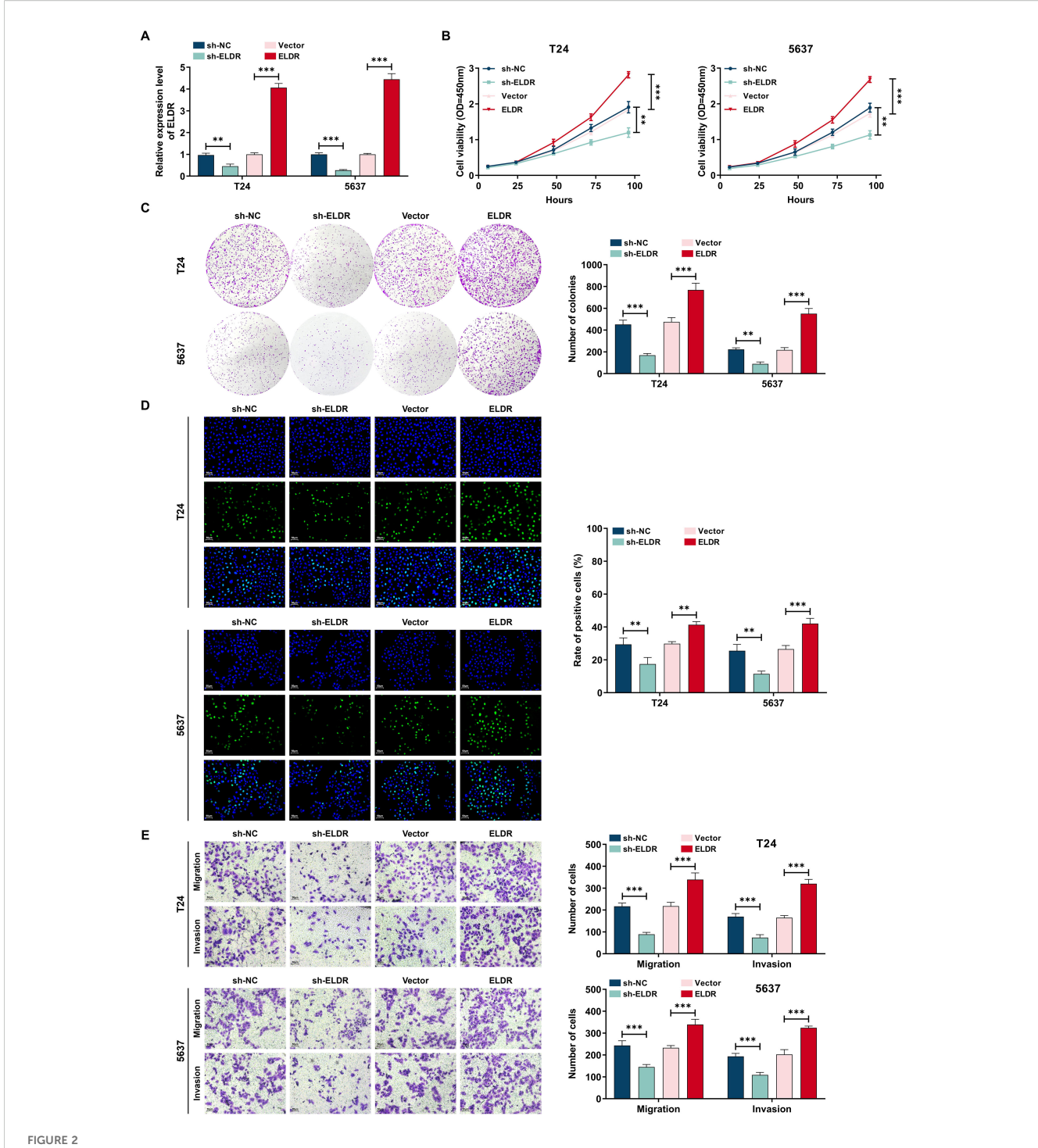
## 3.3 *ELDR* knockdown suppresses tumor growth *in vivo*

Next, to further assess the effects of *ELDR* on BCa tumorigenesis *in vivo*, we established subcutaneous xenograft models by injecting nude mice with T24 cells stably expressing control shRNA or two independent shRNAs targeting *ELDR* (FigureS 3A, B). Tumors derived from sh-*ELDR*-infected T24 cells exhibited significantly reduced growth rates and smaller volumes compared to those from control shRNA-infected cells (Figures 3C-E). Additionally, immunohistochemical (IHC) analysis revealed a striking reduction in the expression of the proliferation marker Ki67 in tumors from the sh-*ELDR* group compared to the control group (Figure 3F). Collectively, these results demonstrate that *ELDR* inhibition could suppress BCa tumor growth *in vivo*.

## 3.4 *ELDR* localizes to the cytoplasm and functions as a miR-1343-3p sponge

We explored the molecular mechanisms of *ELDR*-mediated BCa tumorigenesis. Considering that the mechanisms and functions are dictated by subcellular localization, we first defined the compartmental distribution of ELDR (25). Bioinformatics prediction using the iLoc-lncRNA database indicated its predominant cytoplasmic accumulation (Figure 4A). This distribution was confirmed experimentally through subcellular fractionation and qRT-PCR in both T24 and 5637 cells, with fraction purity verified by immunoblotting for GAPDH (cytoplasmic marker) and PCNA (nuclear marker) (Figures 4B, C). Based on the established role of cytoplasmic noncoding RNAs in miRNA sequestration and target derepression, we hypothesized that *ELDR* acts as a molecular sponge for specific miRNAs to regulate downstream oncogenic genes (26).

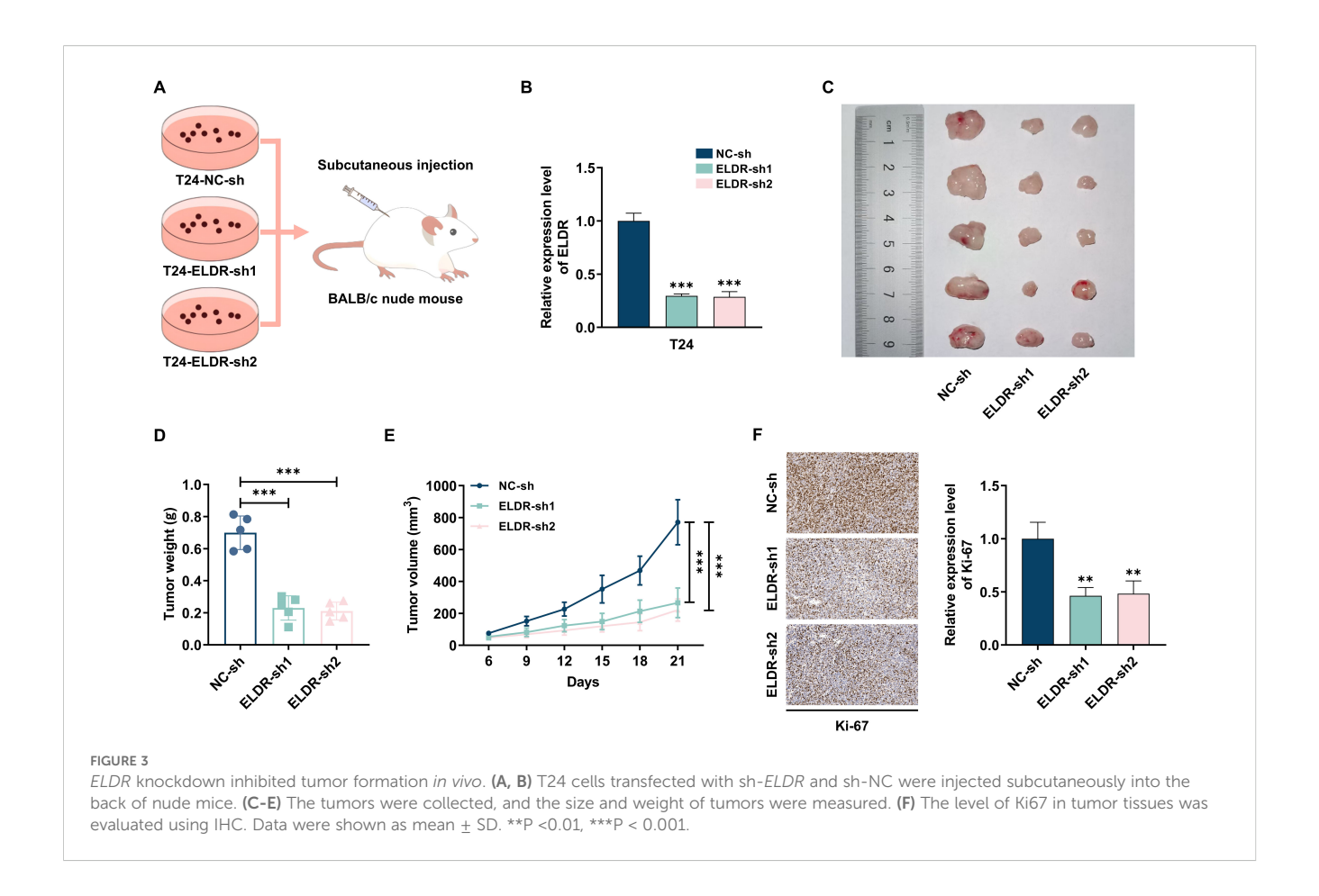
To identify the underlying mechanism, potential miRNAs binding to *ELDR* were predicted using the starBase, miRDB, lncRNASNP2, and LncBook databases. By intersecting the four databases, we obtained two predicted miRNAs, miR-1343-3p and miR-6783-3p (Figure 4D). We performed qRT-PCR assays to confirm that miR-1343-3p is the direct downstream target of *ELDR*, as *ELDR* overexpression decreased miR-1343-3p levels while its knockdown upregulated them in both cell lines (Figure 4E). To ascertain the interaction between *ELDR* and miR-



FLDR promotes cell proliferation, colony formation, migration, and invasion in BCa cells. T24 and 5637 were transfected with sh-NC, sh-ELDR, pcDNA3.1 or pc-ELDR. (A) ELDR expression was assessed using qRT-PCR assay. (B-D) CCK-8, colony formation, and EDU assays were employed to determine cell proliferation. (E) Cell migration and invasion were detected using transwell assay. Data were shown as mean  $\pm$  SD. \*\*P <0.01, \*\*\*P < 0.001.

1343-3p, we predicted their binding sites using starBase and constructed the wild-type (WT) and mutant (MUT) *ELDR* luciferase reporter genes respectively. We performed the dual-luciferase assays, and the results of dual-luciferase indicated that the luciferase activity of *ELDR*-WT, but not MUT, was markedly attenuated by miR-1343-3p (Figure 4F, Supplementary Figure S1A). Furthermore, *ELDR* expression levels were significantly higher than

those of miR-1343-3p in both cell lines, supporting its efficacy as a competing endogenous RNA in binding miR-1343-3p (Supplementary Figure S1B). It is well established that lncRNA-miRNA interactions depend on the AGO2 complex; therefore, we performed AGO2-RIP assays in both cell lines, which revealed that *ELDR* directly bound to the AGO2-containing miR-1343-3p ribonucleoprotein complex, but this interaction was obviously



reduced upon inhibition of miR-1343-3p (Figure 4G, Supplementary Figure S1C). Subsequently, MS2-RIP assays demonstrated that endogenous miR-1343-3p was enriched by the MS2-ELDR-WT complex, further validating endogenous binding between ELDR and miR-1343-3p (Figures 4H, I). Besides, in BCa tissues from our in-house cohort, the miR-1343-3p expression level was significantly downregulated compared to paired adjacent normal tissues, and correlation analyses revealed that the ELDR expression level was negatively correlated with miR-1343-3p (Supplementary Figures S1D, E, Supplementary Table S1). Altogether, ELDR localized in the cytoplasm sponges miR-1343-3p to suppress its expression in BCa.

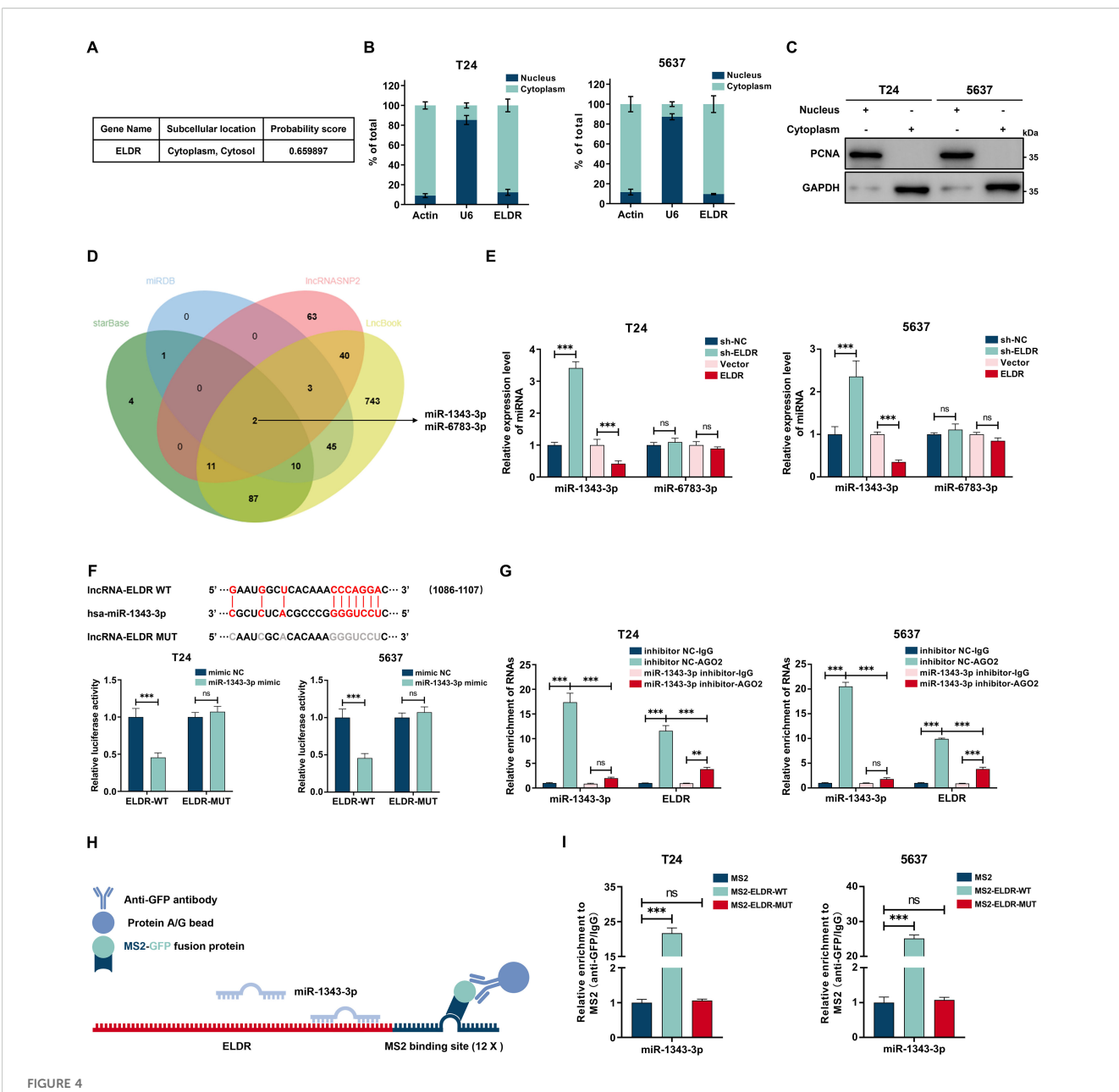
## 3.5 MiR-1343-3p inhibitor rescued malignant phenotypes suppressed by *ELDR* knockdown in BCa cells

To explore the functional significance of the *ELDR*/miR-1343-3p axis in BCa progression, we allocated T24 and 5637 cells into three experimental groups: shRNA negative control (sh-NC), *ELDR*-knockdown (sh-*ELDR*), and combined *ELDR*-knockdown with miR-1343-3p inhibitor (sh-*ELDR* + miR-1343-3p inhibitor), followed by CCK-8, colony formation, EdU and transwell assays (Figures 5A). As displayed in Figures 5B-E, *ELDR* knockdown

markedly suppressed proliferation, colony formation, migration, and invasion capacities in both cell lines. Conversely, the miR-1343-3p inhibitor attenuated these suppressive effects, rescuing malignant phenotypes. Collectively, *ELDR* functions as a driver in BCa progression by targeting miR-1343-3p.

#### 3.6 *ELDR* functions as a ceRNA for miR-1343-3p to upregulate TRIM44 expression

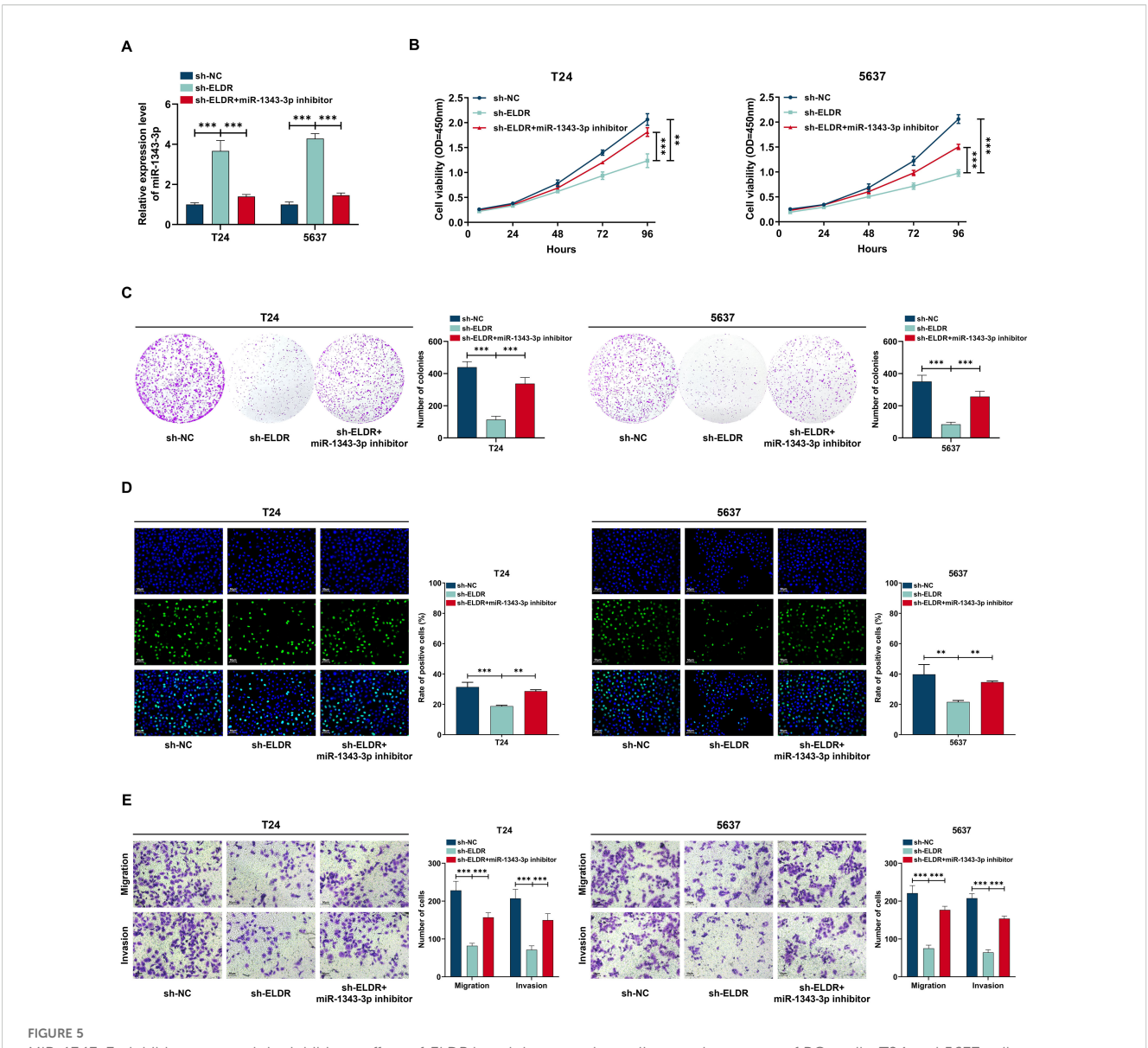
Given that miRNAs exert their function via regulating the expression of target genes, we employed four bioinformatic databases—starBase, miRDB, miRTarBase, and TargetScan—to predict candidate targets of miR-1343-3p. As shown in Figure 6A, sixteen targets overlapped in the prediction results of these four databases. We performed qRT-PCR assays, and the results of showed that only the expression level of *TRIM44* mRNA was sharply decreased after treatment with miR-1343-3p mimic in T24 and 5637 cells (Supplementary Figure S1F). Conversely, the miR-1343-3p inhibitor promoted the *TRIM44* mRNA expression level in both cell lines (Figure 6B). A similar pattern of expression was observed for the TRIM44 protein by western blot assay (Figure 6C). Subsequently, we confirmed that miR-1343-3p directly bound to the 3'-UTR of *TRIM44* via a dual-luciferase reporter assay. Transfection with the miR-1343-3p mimic



Cytoplasmic *ELDR* acted as a sponge of miR-1343-3p. (A) Subcellular localization of *ELDR* in cells predicted by iLoc-lncRNA databese. (B) The subcellular localization of *ELDR* in T24 (left panel) and 5637 (right panel) cells was determined by nuclear and cytoplasmic fractionation experiment followed by RT-qPCR analysis. (C) The nuclear and cytoplasmic fractionations as described in B were subjected to immunoblotting analysis. (D) Online predicting the *ELDR* target miRNAs. Venn gram showed the intersection miRNAs. (E) qRT-PCR assays were performed to screen target miRNAs of *ELDR* by silencing or overexpressing *ELDR* in BCa cell lines. (F) Online predicting of the interaction sites between *ELDR* and miR-1343-3p, T24 and 5637 cells were transfected with reporters containing wild-type or mutated *ELDR* in the presence or absence of negative control miRNA mimic or miR-1343-3p mimic followed by luciferase activity measurement. (G) RIP assays were used to pulldown the endogenous RNA associated with AGO2 in T24 and 5637 cells transfected with miR-1343-3p inhibitor or inhibitor NC, and the relative levels of *ELDR* and miR-1343-3p were measured and normalized according to the result in IgG group. (H) Schematic delineating the strategy of MS2-RIP. (I) MS2-RIP assays in T24 and 5637 cells followed by qRT-PCR examining the endogenous binding between *ELDR* and miR-1343-3p. Data were shown as mean ± SD, \*\*P < 0.01, \*\*\*P < 0.001.

significantly suppressed luciferase activity driven by the wild-type (WT) *TRIM44* 3'-UTR reporters relative to the miR-NC control in both cell lines, whereas activity of the mutant (MUT) reporter was unaffected (Figure 6D). We also detected TRIM44 expression level in our in-house cohort using western blot and qRT-PCR assays. The result showed that TRIM44 was markedly upregulated in the tumor

tissues compared with paired adjacent normal tissues (Supplementary Figures S1G, SH). Moreover, *TRIM44* mRNA expression level showed a positive relationship with *ELDR* and an inverse association with miR-1343-3p (Supplementary Figures SI, SJ, Supplementary Table S1). Finally, silencing *ELDR* expression substantially diminished TRIM44 protein levels in both cell lines,



MiR-1343-3p inhibitor reversed the inhibitory effect of *ELDR* knockdown on the malignant phenotypes of BCa cells. T24 and 5637 cells were classified into: sh-NC group, sh-*ELDR*+miR-1343-3p inhibitor group. (**A**) MiR-1343-3p was determined using qRT-PCR assay. (**B-D**) Cell proliferation was determined using CCK-8 assay, colony formation, and EDU assay. (**E**) Cell migration and invasion were determined using transwell assay. Data were expressed as mean  $\pm$  SD, \*\*P <0.01, \*\*\*P < 0.001.

whereas this reduction was reversed by the miR-1343-3p inhibitor (Figure 6E). In summary, *ELDR* promotes TRIM44 expression via sponging miR-1343-3p.

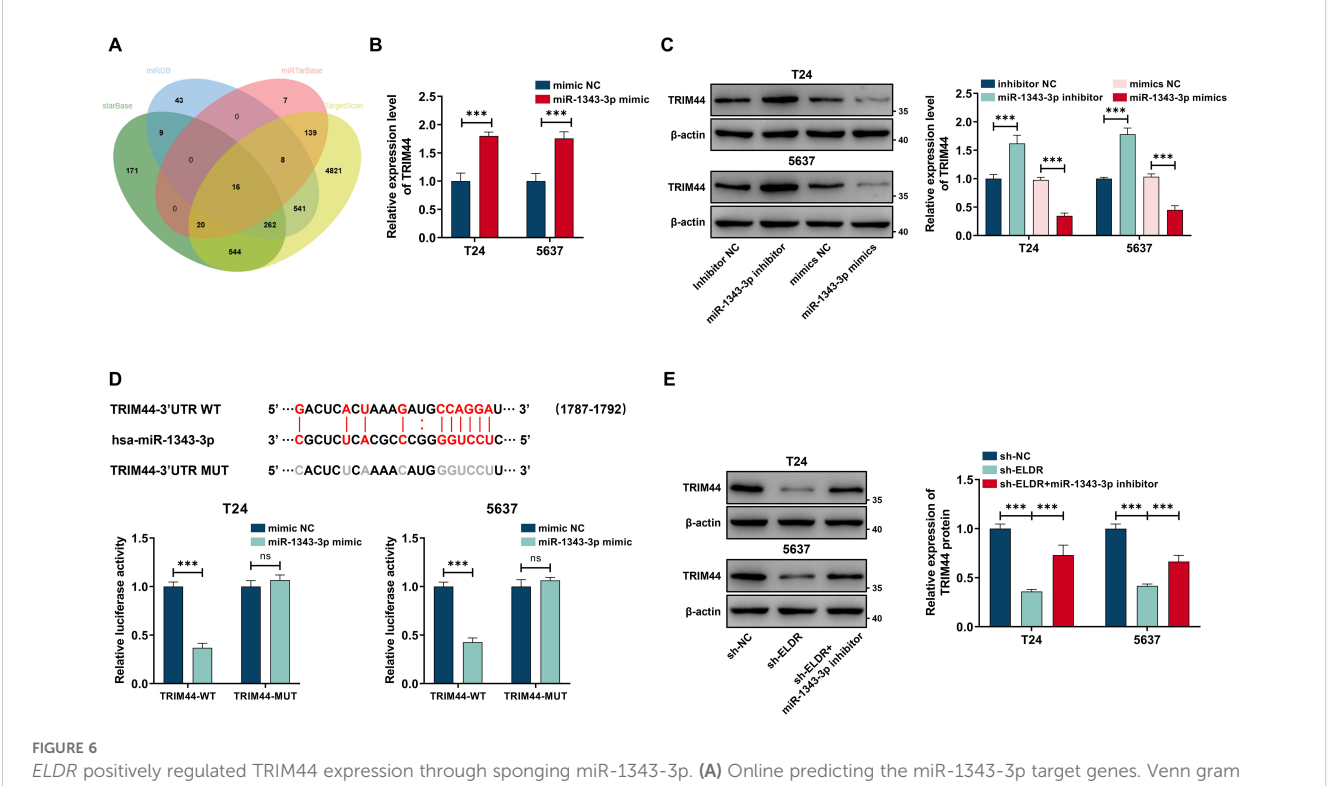
# 3.7 TRIM44 overexpression rescued the inhibition of *ELDR* knockdown on the malignant phenotypes of BCa cells

To determine whether *TRIM44* mediates *ELDR* oncogenic function in BCa, we performed rescue experiments via restoring TRIM44 expression. *ELDR* knockdown significantly reduced TRIM44 protein levels in T24 and 5637 cells, an effect rescued by

pcDNA3.1-*TRIM44* transfection (Figure 7A). Subsequent functional assays revealed that silencing *ELDR* inhibited BCa cell proliferation, colony formation, migration, and invasion in both cell lines (Figures 7B-E). Notably, TRIM44 restoration abolished *ELDR*-silencing-induced suppression of these malignant phenotypes (Figures 7B-E). Collectively, TRIM44 overexpression rescues the inhibitory effects of *ELDR* depletion on BCa oncogenicity.

#### 4 Discussion

As the primary genitourinary malignancy, the prognosis of BCa remains poor due to a lack of effective diagnostic biomarkers and



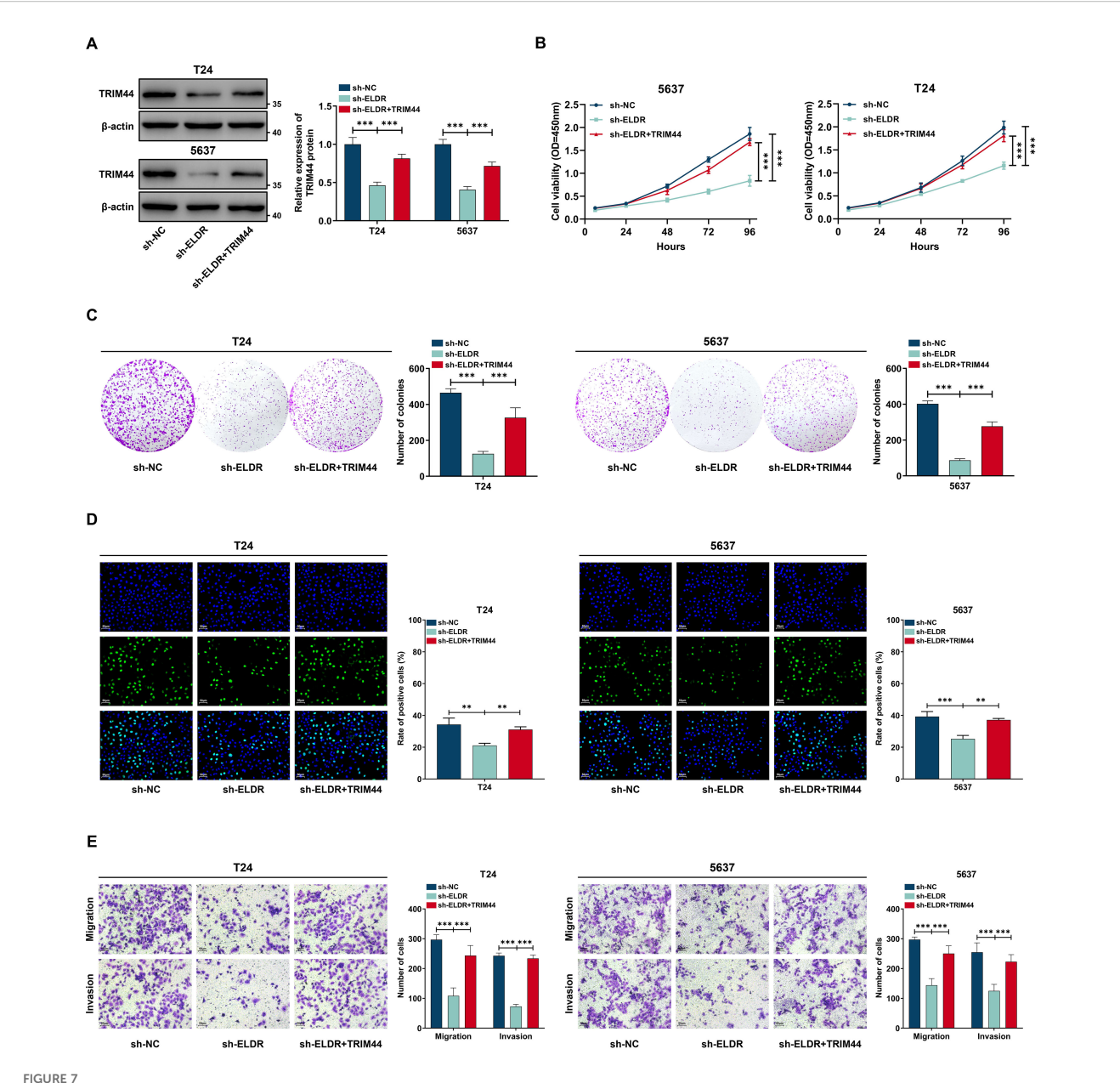
ELDR positively regulated TRIM44 expression through sponging miR-1343-3p. (A) Online predicting the miR-1343-3p target genes. Venn gram showed the intersection genes. (B) TRIM44 mRNA expression in T24 and 5637 cells after miR-1343-3p overexpression was determined using qRT-PCR. (C) TRIM44 proteins levels after transfection of miR-1343-3p mimic and inhibitor in the above two cell lines. (D) Online predicting of the interaction sites between miR-1343-3p and TRIM44, and luciferase reporter assays demonstrated TRIM44 was a direct target of miR-1343-3p. (E) TRIM44 expression in 5637 and T24 cells after sh-ELDR transfection or sh-ELDR and miR-1343-3p inhibitor co-transfection was detected by western blot. Data were expressed as mean ± SD, \*\*P < 0.01, \*\*\*P < 0.001.

therapeutic drugs (27). It has been reported that abnormal proliferation is the main reason for the occurrence and malignant progression of BCa (28). Therefore, there is an urgent need to better understand the underlying molecular mechanisms of BCa progression and improve the survival of BCa patients. LncRNAs have received increasing attention due to their important roles in the development and progression of human cancers, including BCa (29-32). For example, TUG1 (33) and SNHG16 (34) showed overexpression in BCa tumor tissues and served as bad predictors of overall survival. However, the exact role of lncRNAs in BCa remains poorly understood. A comprehensive understanding of the mechanisms of lncRNAs will help reveal promising biomarkers and therapeutic targets for BCa patients. While the ceRNA paradigm and the oncogenic role of TRIM44 have been documented in various cancer types, the upstream regulators that dictate TRIM44 expression in BCa remain poorly characterized.

In this study, we focused our attention on a lncRNA *ELDR* that has not been reported in BCa and whose function is still unclear. Our work provides the first evidence that *ELDR* functions as a key oncogenic lncRNA in BCa by operating as a competitive endogenous RNA (ceRNA). We found that the expression level of *ELDR* was obviously upregulated in BCa tissues compared to the paired adjacent normal tissues, correlating with tumor size, invasion depth, TNM stage and poor prognosis in BCa patients. Functional experiments displayed that silencing *ELDR* inhibited the

BCa cell proliferation, colony formation, migration, and invasion, whereas overexpression of *ELDR* showed the opposite effect. The tumor-promoting effect of *ELDR in vivo* was further validated. While other well-characterized oncogenic lncRNAs in BCa, such as *UCA1* and *MALAT1*, have been associated with specific processes like chemoresistance and metastasis, respectively, our date defines a distinct role for *ELDR*. We demonstrate that *ELDR* directly sequesters miR-1343-3p, which in turn leads to the derepression of its target oncogene, *TRIM44*. These results motivate us to further explore the biological mechanism of *ELDR* in BCa.

TRIM44, a member of the tripartite motif (TRIM) family E3 ubiquitin ligases, is recognized for its involvement in protein stability regulation and signal transduction (35, 36). Accumulating evidence indicates that the crucial roles of TRIM44 in the development of various types of malignant tumors. TRIM44 overexpression was confirmed to be associated with the malignant phenotype in gastric cancer (37), lung adenocarcinoma (38), and ovarian cancer (22). The precise molecular effects triggered by the upregulation of TRIM44 in bladder cancer require further investigation. our study provides the first evidence of TRIM44 dysregulation in BCa. Moreover, TRIM44 expression was positively correlated with that of ELDR. Importantly, the inhibitory effect of ELDR silencing on the BCa malignant phenotype were significantly attenuated in the presence of TRIM44 overexpression. Based on these results, we concluded

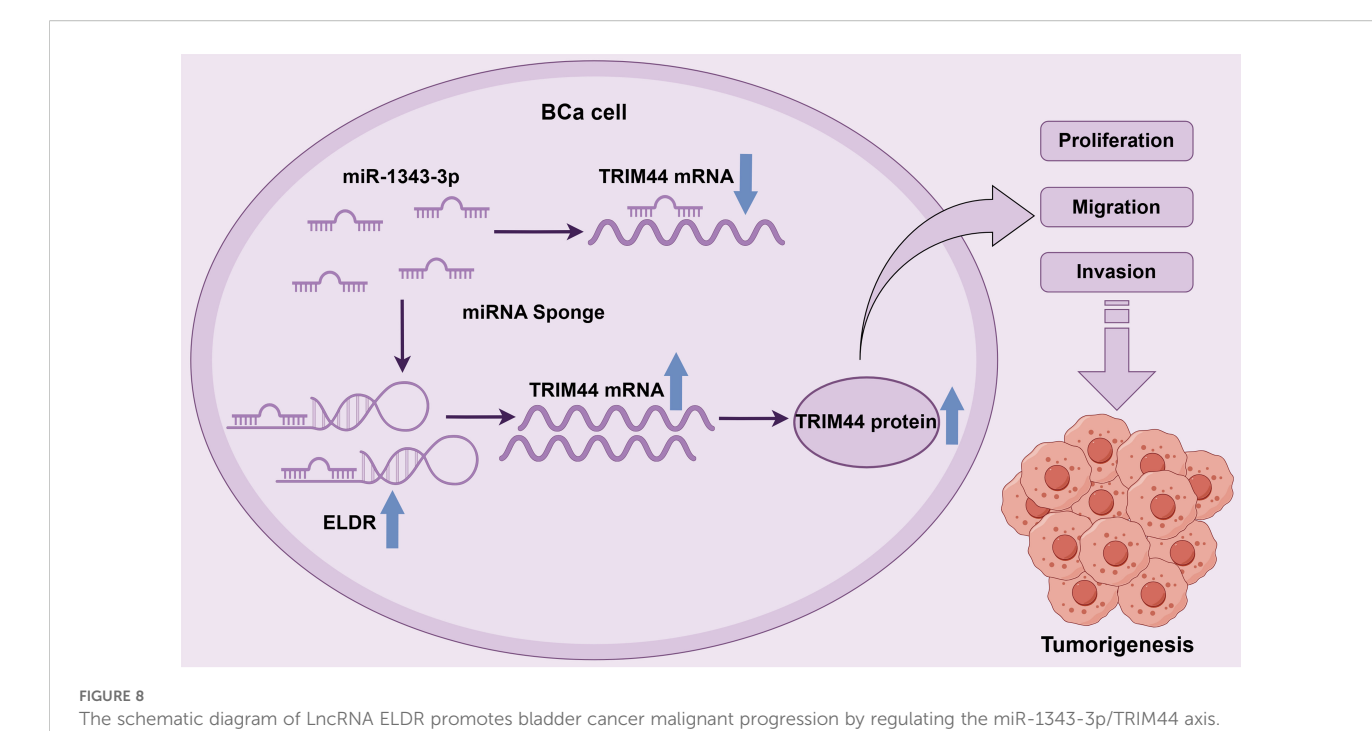


TRIM44 overexpression reversed the inhibitory effect of *ELDR* knockdown on the malignant phenotypes of BCa cells. T24 and 5637 cells were classified into: sh-NC group, sh-*ELDR* group, and sh-*ELDR*+TRIM44 group. (A) Western blot was employed to asses TRIM44 level in T24 and 5637 cells. (B-D) CCK-8 assay, colony information assay, and EDU assay were employed to determine cell proliferation. (E) Cell migration and invasion were determined using transwell assay. Data were expressed as mean  $\pm$  SD, \*\*P < 0.01, \*\*\*P < 0.001.

that ELDR promotes the progression of BCa, at least to some extent, by stimulating the expression of TRIM44. There is already a lot of proof that TRIM44 makes the PI3K protein more stable and speeds up the PI3K/AKT signaling pathways in different malignancies. This suggests that TRIM44 overexpression caused by *ELDR* probably acts in bladder cancer by making this essential cancercausing pathway work too hard. This potential association provides a plausible explanation for the enhanced growth capacity observed in *ELDR*-overexpressing cells. Concurrently, the potent promigration and invasion phenotypes induced by *ELDR* strongly suggest its involvement in regulating epithelial-mesenchymal

transition (EMT)—a core mechanism of cancer metastasis. Future research focusing on this pathway's effects on key EMT transcription factors and biomarkers (such as E-cadherin, N-cadherin, and vimentin) will be crucial for comprehensively elucidating its role in bladder cancer dissemination.

Our findings indicate promising potential for translational applications. From a diagnostic perspective, the substantial increase of *ELDR* in BCa tissues and its association with aggressive disease highlight its potential as a predictive biomarker. Identifying *ELDR* levels in liquid biopsies, such as serum or urine extracellular vesicles, may aid in the creation of non-invasive



diagnostics for early detection and risk assessment. From a therapeutic standpoint, the unique and heightened expression of *ELDR* in malignancies renders it a compelling target for targeted therapies. Targeting lncRNAs poses technical challenges; however, innovative methodologies, including the application of antisense oligonucleotides (ASOs) or small interfering RNAs (siRNAs) specifically engineered to inhibit *ELDR*, may provide a novel and precise therapeutic approach to disrupt this carcinogenic pathway.

It must be acknowledged that this study has limitations. First, our clinical relevance analysis is based solely on a single-center cohort with limited sample size. To establish the post-rain value of *ELDR*, validation through independent, multicenter, large-scale prospective cohorts is essential. Second, although *in vitro* and *in vivo* data strongly support the functional role of the *ELDR*/miR-1343-3p/*TRIM44* axis, the direct clinical utility of *ELDR* and its feasibility for patient treatment remain to be verified. Finally, confirmatory validation of the proposed downstream pathways—particularly the direct activation mechanism of the PI3K/AKT pathway and the role of TRIM44 in inducing epithelial-mesenchymal transition (EMT) in bladder cancer—has become the core focus of our current research.

Collectively, these findings delineate the *ELDR*/miR-1343-3p/ *TRIM44* axis as a functionally independent pathway that expands the known regulatory network of lncRNAs in bladder cancer pathogenesis (Figure 8).

#### Data availability statement

The original contributions presented in the study are included in the article/Supplementary Material. Further inquiries can be directed to the corresponding authors.

#### **Ethics statement**

The studies involving humans were approved by the Medical Ethics Committee of the First Affiliated Hospital of Chongqing Medical University. The studies were conducted in accordance with the local legislation and institutional requirements. The participants provided their written informed consent to participate in this study. The animal study was approved by Chongqing Medical University Experimental Animal Center. The study was conducted in accordance with the local legislation and institutional requirements.

#### **Author contributions**

XH: Data curation, Formal Analysis, Methodology, Investigation, Writing – review & editing. TX: Writing – review & editing, Formal Analysis, Data curation, Validation, Funding acquisition. XX: Methodology, Writing – review & editing, Funding acquisition, Supervision, Project administration. YM: Methodology, Visualization, Data curation, Formal Analysis, Investigation, Conceptualization, Writing – original draft.

#### **Funding**

The author(s) declare financial support was received for the research and/or publication of this article. This work was supported by the Fuling District Science and Technology Research Program (FLKJ.2024AAN3066), National Natural Science Foundation of China (82372439); National Key Research and Development Program of China (2023YFC3604404, 2023YFC3604405).

#### Conflict of interest

The authors declare that the research was conducted in the absence of any commercial or financial relationships that could be construed as a potential conflict of interest.

#### Generative AI statement

The author(s) declare that no Generative AI was used in the creation of this manuscript.

Any alternative text (alt text) provided alongside figures in this article has been generated by Frontiers with the support of artificial intelligence and reasonable efforts have been made to ensure accuracy, including review by the authors wherever possible. If you identify any issues, please contact us.

#### Publisher's note

All claims expressed in this article are solely those of the authors and do not necessarily represent those of their affiliated organizations, or those of the publisher, the editors and the reviewers. Any product that may be evaluated in this article, or claim that may be made by its manufacturer, is not guaranteed or endorsed by the publisher.

#### Supplementary material

The Supplementary Material for this article can be found online at: https://www.frontiersin.org/articles/10.3389/fonc.2025.1685792/full#supplementary-material

#### References

- 1. Leeming RC, Karagas MR, Zens MS, Schned AR, Seigne JD, Passarelli MN. Bladder cancer risk variants and overall and disease-specific survival in two independent cohorts. *BJU Int.* (2022) 129:309–11. doi: 10.1111/bju.15640
- 2. Prout GRJr., Wesley MN, Greenberg RS, Chen VW, Brown CC, Miller AW, et al. Bladder cancer: race differences in extent of disease at diagnosis. *Cancer*. (2000) 89:1349–58. doi: 10.1002/1097-0142(20000915)89:6<1349::AID-CNCR20>3.0.CO;2-D
- 3. Ploeg M, Aben KK, Kiemeney LA. The present and future burden of urinary bladder cancer in the world. World J Urol. (2009) 27:289–93. doi: 10.1007/s00345-009-0383-3
- 4. Iyer MK, Niknafs YS, Malik R, Singhal U, Sahu A, Hosono Y, et al. The landscape of long noncoding RNAs in the human transcriptome. Nat Genet. (2015) 47:199–208. doi: 10.1038/ng.3192
- 5. Schloßhauer JL, Shamloo S, Schamrin K, Imig J. Dual CRISPR-interference strategy for targeting synthetic lethal interactions between non-coding RNAs in cancer cells. *J Vis Exp.* (2025). doi: 10.3791/67752
- 6. Shi M, Zhang R, Lyu H, Xiao S, Guo D, Zhang Q, et al. Long non-coding RNAs: Emerging regulators of invasion and metastasis in pancreatic cancer. J Adv Res. (2025). doi: 10.1016/j.jare.2025.02.001
- 7. Liu P, Fan B, Othmane B, Hu J, Li H, Cui Y, et al. m(6)A-induced lncDBET promotes the Malignant progression of bladder cancer through FABP5-mediated lipid metabolism. *Theranostics*. (2022) 12:6291–307. doi: 10.7150/thno.71456
- 8. Dai C, Li Q, Wang L, Zhang J, Yang S, Zhang X. LncRNA TRPM2-AS promotes cell proliferation, migration, and invasion by regulating the miR-195-5p/COP1 axis in bladder cancer. *Naunyn Schmiedebergs Arch Pharmacol.* (2025). doi: 10.1007/s00210-025-04377-4
- 9. Xue ST, Cao SQ, Ding JC, Li WJ, Hu GS, Zheng JC, et al. LncRNA LUESCC promotes esophageal squamous cell carcinoma by targeting the miR-6785-5p/NRSN2 axis. *Cell Mol Life Sci.* (2024) 81:121. doi: 10.1007/s00018-024-05172-9
- 10. Sheng J, Luo Y, Lv E, Liang H, Tao H, Yu C, et al. LINC01980 induced by TGF-beta promotes hepatocellular carcinoma metastasis via miR-376b-5p/E2F5 axis. *Cell Signal.* (2023) 112:110923. doi: 10.1016/j.cellsig.2023.110923
- 11. Sur S, Nakanishi H, Steele R, Zhang D, Varvares MA, Ray RB. Long non-coding RNA ELDR enhances oral cancer growth by promoting ILF3-cyclin E1 signaling. *EMBO Rep.* (2020) 21:e51042. doi: 10.15252/embr.202051042
- 12. Zhao X, Guo X, Jiao D, Zhu J, Xiao H, Yang Y, et al. Analysis of the expression profile of serum exosomal lncRNA in breast cancer patients. *Ann Transl Med.* (2021) 9:1382. doi: 10.21037/atm-21-3483
- 13. Bartel DP. MicroRNAs: genomics, biogenesis, mechanism, and function. *Cell.* (2004) 116:281–97. doi: 10.1016/S0092-8674(04)00045-5
- 14. Nikkhah O, Einollahi B, Asadi M, Heiat M, Hushmandi K. Gene network changes after exposure to nanoliposomes containing antisense miR-21 and miR-373 in bladder cancer Cells: An *in vitro* model study. *Biochem Biophys Rep.* (2025) 42:102041. doi: 10.1016/j.bbrep.2025.102041
- 15. Yin C, Liufu C, Ye S, Zhu T, Jiang J, Wang M, et al. Tumor-derived exosomal KPNA2 activates fibroblasts and interacts with KIFC1 to promote bladder cancer progression, a process inhibited by miR-26b-5p. *Cell Mol Biol Lett.* (2025) 30:20. doi: 10.1186/s11658-025-00687-w
- 16. Zhang C, Yu H, Bai X, Zhou X, Feng Z, Li Y, et al. MiR-15b-3p weakens bicalutamide sensitivity in prostate cancer via targeting KLF2 to suppress ferroptosis. *J Cancer.* (2024) 15:2306–17. doi: 10.7150/jca.92379

- $17.~{\rm Xu}$ L, Yu S, Li D. miR-1343-3p, mediated by LncRNA ASMTL-AS1, induces ferroptosis in osteosarcoma progression by targeting TYRO3.  $\it Gene.~(2025)~963:149547.$  doi: 10.1016/j.gene.2025.149547
- 18. Zhang Y, Wang X, Liu W, Lei T, Qiao T, Feng W, et al. CircGLIS3 promotes gastric cancer progression by regulating the miR-1343-3p/PGK1 pathway and inhibiting vimentin phosphorylation. *J Transl Med.* (2024) 22:251. doi: 10.1186/s12967-023-04625-2
- 19. Wang X, Zhang Z, Cao X. Salidroside inhibited the proliferation of gastric cancer cells through up-regulating tumor suppressor miR-1343-3p and down-regulating MAP3K6/MMP24 signal molecules. *Cancer Biol Ther.* (2024) 25:2322206. doi: 10.1080/15384047.2024.2322206
- 20. Lai C, Hu Z, Hu J, Li Z, Li L, Liu M, et al. Screening model for bladder cancer early detection with serum miRNAs based on machine learning: A mixed-cohort study based on 16,189 participants. *Cancer Med.* (2024) 13:e70338. doi: 10.1002/cam4.70338
- 21. Yu XZ, Yuan JL, Ye H, Yi K, Qie MR, Hou MM. TRIM44 facilitates ovarian cancer proliferation, migration, and invasion by inhibiting FRK. *Neoplasma*. (2021) 68:751–9. doi: 10.4149/neo\_2021\_201128N1285
- 22. Yu Y, Li S, Sun J, Wang Y, Xie L, Guo Y, et al. Overexpression of TRIM44 mediates the NF-kB pathway to promote the progression of ovarian cancer. *Genes Genomics*. (2024) 46:689–99. doi: 10.1007/s13258-024-01517-7
- 23. Zhou S, Wu C, Tang Q, Zhou X, He B, Chang P, et al. Silencing LINC00491 inhibits prostate cancer development through the miR-384/TRIM44 axis. *J Biochem Mol Toxicol.* (2023) 37:e23370. doi: 10.1002/jbt.23370
- 24. Yamada Y, Kimura N, Maki K, Hakozaki Y, Urabe F, Kimura S, et al. The roles of tripartite motif proteins in urological cancers: A systematic review. *Cancers (Basel)*. (2025) 17:2367. doi: 10.3390/cancers17142367
- 25. Chen LL. Linking long noncoding RNA localization and function. *Trends Biochem Sci.* (2016) 41:761–72. doi: 10.1016/j.tibs.2016.07.003
- 26. Svoronos AA, Engelman DM, Slack FJ. OncomiR or tumor suppressor? The duplicity of microRNAs in cancer. *Cancer Res.* (2016) 76:3666–70. doi: 10.1158/0008-5472.CAN-16-0359
- 27. Kurtova AV, Xiao J, Mo Q, Pazhanisamy S, Krasnow R, Lerner SP, et al. Blocking PGE2-induced tumour repopulation abrogates bladder cancer chemoresistance. *Nature*. (2015) 517:209–13. doi: 10.1038/nature14034
- 28. Olsson AY, Feber A, Edwards S, Te Poele R, Giddings I, Merson S, et al. Role of E2F3 expression in modulating cellular proliferation rate in human bladder and prostate cancer cells. *Oncogene*. (2007) 26:1028–37. doi: 10.1038/sj.onc.1209854
- 29. Ulitsky I, Bartel DP. lincRNAs: genomics, evolution, and mechanisms. Cell. (2013) 154:26–46. doi: 10.1016/j.cell.2013.06.020
- 30. Ma CC, Xiong Z, Zhu GN, Wang C, Zong G, Wang HL, et al. Long non-coding RNA ATB promotes glioma Malignancy by negatively regulating miR-200a. *J Exp Clin Cancer Res.* (2016) 35:90. doi: 10.1186/s13046-016-0367-2
- 31. Xiong J, Liu Y, Jiang L, Zeng Y, Tang W. High expression of long non-coding RNA lncRNA-ATB is correlated with metastases and promotes cell migration and invasion in renal cell carcinoma. *Jpn J Clin Oncol.* (2016) 46:378–84. doi: 10.1093/jjco/hyv214
- 32. Ding J, Lu B, Wang J, Wang J, Shi Y, Lian Y, et al. Long non-coding RNA Loc554202 induces apoptosis in colorectal cancer cells via the caspase cleavage cascades. *J Exp Clin Cancer Res.* (2015) 34:100. doi: 10.1186/s13046-015-0217-7

- 33. Yu G, Zhou H, Yao W, Meng L, Lang B. lncRNA TUG1 Promotes Cisplatin Resistance by Regulating CCND2 via Epigenetically Silencing miR-194-5p in Bladder Cancer. *Mol Ther Nucleic Acids.* (2019) 16:257–71. doi: 10.1016/j.omtn.2019.02.017
- 34. Zhou X, Zhang C, Yu H, Feng Z, Bai X, Mei Y, et al. The MEF2A/SNHG16/miR-425-5p/NOTCH2 axis induces gemcitabine resistance by inhibiting ferroptosis in the starving bladder tumor microenvironment. *Cell Signal.* (2024) 122:111337. doi: 10.1016/j.cellsig.2024.111337
- 35. Watanabe M, Hatakeyama S. TRIM proteins and diseases. J Biochem. (2017) 161:135–44. doi:  $10.1093/\mathrm{jb/mvw087}$
- 36. Allen MD, Bycroft M. The solution structure of the ZnF UBP domain of USP33/VDU1. Protein Sci. (2007) 16:2072–5. doi: 10.1110/ps.072967807
- 37. Zhang X, Wu X, Sun Y, Chu Y, Liu F, Chen C. TRIM44 regulates tumor immunity in gastric cancer through LOXL2-dependent extracellular matrix remodeling. *Cell Oncol (Dordr)*. (2023) 46:423–35. doi: 10.1007/s13402-022-00759-5
- 38. Zhang S, Cao M, Yan S, Liu Y, Fan W, Cui Y, et al. TRIM44 promotes BRCA1 functions in HR repair to induce Cisplatin Chemoresistance in Lung Adenocarcinoma by Deubiquitinating FLNA. *Int J Biol Sci.* (2022) 18:2962–79. doi: 10.7150/ijbs.71283